

Adaptive adjoint Monte Carlo simulation for the uncertainty analysis of the impact assessment of a deep radioactive waste repository

M. Magolu monga Made*, O.F. Smidts†, and A. Dubus

Université Libre de Bruxelles, Service de Métrologie Nucléaire, C.P. 165/84; 50, avenue F.D. Roosevelt, B-1050 Brussels, Belgium. magolu@ulb.ac.be, osm@avn.be, adubus@ulb.ac.be

Abstract

In order to take into account uncertainties about the values of the hydro-geological parameters of the rock hosting a deep geological repository, probabilistic methods are used in the risk assessment of radioactive waste repositories. Random generators could be globally invoked twice in adjoint Monte Carlo (AMC) simulation. Once for sampling hydro-geological parameters from known probability density functions (pdf). Next, for each selected set of parameters, random walks could be simulated for the evaluation of concentration of contaminants. With a moderate number of random walks (batch size), AMC method is efficient for computing mean values of concentrations. However, the higher moments of the concentration distribution and the distribution tails are in general not evaluated with accuracy. To cope with these inconveniences, we propose an adaptive AMC method in which the batch size is dynamically increased. The new approach is applied for the accurate assessment of the probability of exceeding some imposed critical concentrations.

KEY WORDS: Migration of radionuclides; transport model; partial differential equations; integral formulation; Adjoint Monte Carlo method; probability distribution function; statistical uncertainty

*Corresponding author. Research supported by NIRAS/ONDRAF, the Belgian Agency for Radioactive Waste Management

†Present address: Association Vinçotte Nuclear; 148, rue Walcourt, B-1070 Brussels, Belgium.

1. Introduction

We address the problem of the risk assessment of radioactive waste repositories in deep geological media. The migration of radionuclide chains are simulated through the advection-dispersion transport equations, (see, e.g., [1,10,19]). Recently, in a series of works, [11]-[15], the boundary value problem involved has been transformed into integral equations which are solved by means of Monte Carlo integration method [5,6]. The resulting method is known as a non-analog adjoint Monte Carlo (AMC) simulation method. With this approach, it is easy to quickly estimate instantaneous or cumulative (integration over the simulation time) concentrations of contaminants at specific local areas of the geological medium, for instance at wells and the interface between two different geological layers. This contrasts with classical numerical (finite difference, finite volume or finite element) methods where the solution is computed at grid-points covering the whole physical domain. This gives rise to both memory and time consuming computations, especially in the case of three-dimensional models, or when a stochastic uncertainty analysis is required in order to take into account the uncertainty of hydro-geological parameters involved [3,4,8,16,18,20].

In probabilistic risk analysis of radioactive waste repository by AMC method, the parameters of the geological medium are sampled from given pdfs. Next, for each sampled set of parameters, random walks are simulated to estimate the mathematical expectation of concentration of contaminants at target points or areas. We have observed that with a moderate batch size (number of random walks), AMC method computes accurate mean values of concentrations. However, a fair representation of the concentration distribution requires high batch sizes. This leads us to propose an adaptive AMC method in which the batch size is dynamically increased during successive simulations. We apply the new method to estimate the probability of exceeding some imposed critical concentration, which could arise from regulatory requirements.

The paper is organized as follows. In Section 2, we summarize the theoretical basis behind AMC approach. Section 3 is devoted to the description of our stochastic uncertainty analysis. Numerical experiments are presented in Section 4. Concluding remarks are drawn in Section 5.

2. Theoretical Background

2.1. Contaminant transport equations

We consider the transport of decay chain of radionuclides in a three-dimensional semi-infinite water saturated porous medium \mathcal{D} bounded above by a surface (plane) \mathcal{S} . The governing equations are following [1,2].

$$\mathcal{L}_i A(\bar{r}', t'; i) = \tilde{S}(\bar{r}', t'; i) \quad \text{in } \mathcal{D} \subset \mathcal{R}^3, \quad 1 \leq i \leq N_r \quad (1)$$

$$\bar{n} \left\{ -\bar{D}(\bar{r}') \bar{\nabla}_{\bar{r}'} A(\bar{r}', t'; i) + \bar{q}(\bar{r}') A(\bar{r}', t'; i) \right\} = \beta(\bar{r}', t'; i) \quad \text{on } \mathcal{S}, \quad 1 \leq i \leq N_r$$

where \bar{n} denotes the outward normal on \mathcal{S} , while

$$\mathcal{L}_i = \left\{ \frac{\partial}{\partial t'} [\omega_i(\bar{r}') \cdot] + \bar{\nabla}_{\bar{r}'} [\bar{q}(\bar{r}') \cdot] - \bar{\nabla}_{\bar{r}'} \left[\bar{D}(\bar{r}') \bar{\nabla}_{\bar{r}'} \cdot \right] + \lambda_i \omega_i(\bar{r}') \cdot \right\} \quad (2)$$

$$\tilde{S}(\bar{r}', t'; i) = S(\bar{r}', t'; i) + \lambda_i \omega_{i-1}(\bar{r}') A(\bar{r}', t'; i-1) \quad (3)$$

$$\omega_i(\bar{r}') = \theta(\bar{r}') R_i(\bar{r}') \quad (4)$$

$$A(\bar{r}', t'; i) = \lambda_i C(\bar{r}', t'; i) \quad (5)$$

$$\overline{\overline{D}}(\bar{r}') = \theta(\bar{r}') \overline{\overline{D}}_H(\bar{r}') = \theta(\bar{r}') \left(\overline{\overline{D}}_m(\bar{r}') + \overline{\overline{D}}_c(\bar{r}') \right) \quad (6)$$

with

$$\begin{aligned} \bar{r}' &= \text{three-dimensional variable } (x', y', z') \\ t' &= \text{time variable} \\ N_r &= \text{number of radionuclides in the chain} \\ C(\bar{r}', t'; i) &= \text{concentration of radionuclide } i \\ A(\bar{r}', t'; i) &= \text{activity of radionuclide } i \\ \theta(\bar{r}') &= \text{porosity} \\ R_i(\bar{r}') &= \text{retardation factor of radionuclide } i \\ \bar{q}(\bar{r}') &= \text{Darcy velocity} \quad (\bar{v}(\bar{r}') = \frac{\bar{q}(\bar{r}')}{\theta(\bar{r}')} = \text{advection velocity}) \\ \lambda_i &= \text{radioactive decay constant of radionuclide } i \\ \overline{\overline{D}}(\bar{r}') &= \text{diffusion-dispersion tensor} \\ \overline{\overline{D}}_H(\bar{r}') &= \text{hydrodynamic diffusion-dispersion tensor} \\ \overline{\overline{D}}_m(\bar{r}') &= \text{molecular diffusion tensor} \\ \overline{\overline{D}}_c(\bar{r}') &= \text{kinematic dispersion tensor} \\ S(\bar{r}', t'; i) &= \text{source term of radionuclide } i \end{aligned}$$

2.2. Integral formulation

The following *adjoint reference equations* are needed.

$$\mathcal{L}_i^* C^*(\bar{r}', t'; i) = \delta(\bar{r}' - \bar{r}) \delta(t' - t) \quad \text{for } i=1, \dots, N_r \quad (7)$$

with

$$\mathcal{L}_i^* = -\omega_i^*(\bar{r}') \frac{\partial}{\partial t'} - \bar{q}^*(\bar{r}') \bar{\nabla}_{r'} \cdot - \bar{\nabla}_{r'} \cdot \left[\overline{\overline{D}}^*(\bar{r}') \bar{\nabla}_{r'} \cdot \right] + \lambda_i \omega_i^*(\bar{r}') \quad (8)$$

where δ denotes the Dirac function. Eqs. (7)-(8) is the adjoint of Eq. (1) divided by λ_i , and modified as follows: $\omega_i(\bar{r}')$, $\bar{q}(\bar{r}')$ and $\overline{\overline{D}}(\bar{r}')$ are replaced by $\omega_i^*(\bar{r}')$, $\bar{q}^*(\bar{r}')$ and $\overline{\overline{D}}^*(\bar{r}')$, respectively. Moreover we assume that a unit pulse source is located at $\bar{r}' = \bar{r}$ at time $t' = t$. The choice of the coefficients in (7)-(8) is guided by efficiency reasons of the Monte Carlo simulation [12,14,15]. The analytical (*adjoint reference*) solution of (7-8) is denoted by $C^*(\bar{r}', t'; i | \bar{r}, t; i)$. By generalizing the mathematical transformations elaborated in [9, pages 206-209], the following Volterra integral equation of the second kind has been obtained in [11] (see also, [14, Appendix B and Eq. (19)]).

$$u_S(\bar{r}) A(\bar{r}, t; i) = Q(\bar{r}, t; i) + \sum_{j=i-1}^i \int_{t-T_0}^t dt' \int_{\overline{\overline{D}}} d\bar{r}' \mathcal{K}(\bar{r}', t'; j | \bar{r}, t; i) u_S(\bar{r}') A(\bar{r}', t'; j) \quad (9)$$

with

$$\begin{aligned}
u_{\mathcal{S}}(\bar{r}) &= \begin{cases} \frac{1}{2} & \bar{r} \in \mathcal{S} \\ 1 & \bar{r} \in \mathcal{D} \end{cases} \\
\bar{\mathcal{D}} &= \mathcal{D} \cup \mathcal{S} \\
T_0 &= \text{total simulation time}
\end{aligned} \tag{10}$$

$$Q(\bar{r}, t; i) = \int_{t-T_0}^t \frac{T_0 - (t - t')}{T_0} dt' \int_{\bar{\mathcal{D}}} C^*(\bar{r}', t'; i | \bar{r}, t; i) \{S(\bar{r}', t'; i) - \delta_2(\bar{r}' - \bar{r}'_{\mathcal{S}}) \beta(\bar{r}', t'; i)\} d\bar{r}' \tag{11}$$

$$\mathcal{K}(\bar{r}', t'; j | \bar{r}, t; i) = K^{j \rightarrow j}(\bar{r}', t'; j | \bar{r}, t; i) \delta_{j,i} + K^{j \rightarrow i}(\bar{r}', t'; j | \bar{r}, t; i) (1 - \delta_{j,i}) \tag{12}$$

where δ_2 and $\delta_{j,i}$ denotes a two-dimensional Dirac function associated to the surface \mathcal{S} and the Kronecker symbol, respectively, while

$$\begin{aligned}
K^{j \rightarrow j}(\bar{r}', t'; j | \bar{r}, t; i) &= K_{\mathcal{D}}(\bar{r}', t'; j | \bar{r}, t; j) + \delta_2(\bar{r}' - \bar{r}'_{\mathcal{S}}) K_{\mathcal{S}}(\bar{r}', t'; j | \bar{r}, t; j) \\
K^{j \rightarrow i}(\bar{r}', t'; j | \bar{r}, t; i) &= \lambda_i \omega_j(\bar{r}') \frac{T_0 - (t - t')}{T_0} C^*(\bar{r}', t'; i | \bar{r}, t; i) \frac{1}{u_{\mathcal{S}}(\bar{r}')}
\end{aligned} \tag{13}$$

with

$$\begin{aligned}
K_{\mathcal{D}}(\bar{r}', t'; j | \bar{r}, t; j) &= \frac{1}{u_{\mathcal{S}} T_0} \left\{ \omega_j(\bar{r}') C^*(\bar{r}', t'; j | \bar{r}, t; j) + [T_0 - (t - t')] \right. \\
&\quad \left. \left[\Delta \omega_j \frac{\partial C^*}{\partial t'} + \Delta \bar{q} \bar{\nabla}_{r'} C^* + \bar{\nabla}_{r'} (\Delta \bar{\bar{D}} \bar{\nabla}_{r'} C^*) - \lambda_j \Delta \omega_j C^* \right] \right\} \tag{14}
\end{aligned}$$

$$K_{\mathcal{S}}(\bar{r}', t'; j | \bar{r}, t; j) = \frac{1}{T_0} [T_0 - (t - t')] [-\bar{n} \bar{\bar{D}}(\bar{r}') \bar{\nabla}_{r'} C^*] \frac{1}{u_{\mathcal{S}}(\bar{r}')} \tag{15}$$

where

$$\begin{aligned}
\Delta \omega_j &= \omega_j(\bar{r}') - \omega_j^* \\
\Delta \bar{q} &= \bar{q}(\bar{r}') - \bar{q}^* \\
\Delta \bar{\bar{D}} &= \bar{\bar{D}}(\bar{r}') - \bar{\bar{D}}^*
\end{aligned} \tag{16}$$

2.3. Monte Carlo methods

For simplicity, we drop the radionuclide index i . The integral equation (9)-(16), divided by λ_i , may be formally written as:

$$C(\bar{r}, t) = Q(\bar{r}, t) + \int dt' \int d\bar{r}' K(\bar{r}', t' | \bar{r}, t) C(\bar{r}', t') \tag{17}$$

or, in abbreviated form:

$$C = Q + \kappa C \tag{18}$$

where κ stands for the appropriate integral operator. In practice, one evaluates the functional

$$J = \int dt \int d\bar{r} \varphi(\bar{r}, t) C(\bar{r}, t) \quad (19)$$

where $\varphi(\bar{r}, t)$ denotes the *pay-off function* [6,13]. We report below examples of pay-off functions which play a key role in the risk assessment of radioactive waste repositories.

1. $\varphi(\bar{r}, t) = \delta(\bar{r} - \bar{P}_k) \delta(t - t_\mu)$ with $\bar{P}_k = \bar{r}_k = (x_k, y_k, z_k)$. J corresponds to the concentration at time t_μ at location \bar{P}_k .

2. $\varphi(\bar{r}, t) = \delta(\bar{r} - \bar{P}_k) H_{[0, T_0]}(t)$ where $H_{[0, T_0]}(t) = 1$ inside $[0, T_0]$ and 0 outside $[0, T_0]$. J gives the cumulative concentration from $t = 0$ to $t = T_0$ at \bar{P}_k .

3. $\varphi(\bar{r}, t) = \delta_2(\bar{r} - \bar{r}_{\mathcal{S}_\ell}) H_{[0, T_0]}(t)$ where δ_2 denotes a two-dimensional Dirac function associated to the surface \mathcal{S}_ℓ . J yields the concentration accumulated on \mathcal{S}_ℓ during the time interval $[0, T_0]$.

By expanding (18) into a Neumann series one obtains:

$$C = (I - \kappa)^{-1} Q = Q + \kappa Q + \kappa^2 Q + \kappa^3 Q + \dots \quad (20)$$

where I stands for the identity operator. Hence it follows that

$$C(\bar{r}, t) = \sum_{j=0}^{\infty} C_j(\bar{r}, t) \quad (21)$$

with

$$\begin{aligned} C_0(\bar{r}, t) &= Q(\bar{r}, t) \\ C_j(\bar{r}, t) &= \kappa C_{j-1}(\bar{r}', t') \\ &= \int dt' \int d\bar{r}' K(\bar{r}', t' | \bar{r}, t) C_{j-1}(\bar{r}', t') \quad . \end{aligned} \quad (22)$$

Therefore,

$$J = \sum_{j=0}^{\infty} J_j \quad (23)$$

where

$$J_j = \int dt \int d\bar{r} f(\bar{r}, t) C_j(\bar{r}, t) \quad . \quad (24)$$

In practice, each integral that appears in (24) is computed by means of classical Monte Carlo integration method [5,6]. A limited number of Neumann terms ($N_L \leq 20$) is in general sufficient to obtain accurate estimate [7].

3. A stochastic uncertainty analysis

A very important issue in any risk assessment analysis is the effects of the hydro-geological parameters uncertainties on the mathematical models. Our analysis is confined to the uncertainties on the value of the retardation factors.

3.1. Uncertainty of retardation factors

In our model the retardation factor is constant per geological layer. For any radionuclide j one has that [2,4]:

$$R_j = 1 + \frac{\rho_b}{\theta} K_d^{(j)} \quad (25)$$

where ρ_b , θ , and $K_d^{(j)}$ denote the bulk density of the solid phase, the porosity, and the sorption distribution coefficient, respectively. The coefficient $K_d^{(j)}$, which is highly dependent on the composition of the porous medium, the type of the radionuclide, and a series of chemical conditions like pH, is mainly responsible for the uncertainty on the retardation factor. It is widely admitted that $K_d^{(j)}$ is log-normally (natural logarithm) distributed (say, $Y^{(j)} = \ln K_d^{(j)}$ is a normal distribution) [8]. This gives rise to the following pdf for R_j :

$$f(R_j) = \frac{1}{\sqrt{2\pi}\sigma_j R_j} \exp\left(-\frac{(\ln R_j - \mu_j)^2}{2\sigma_j^2}\right) \quad (26)$$

where μ_j and σ_j stand for the mean and the standard deviation of the log-normal pdf involved. For later use, we report in Table 1 some values for a geological medium made of clay and sand.

Table 1: Means (μ) and standard deviations (σ) of the log-normal pdfs for the retardation factors of ^{240}Pu and ^{236}U in clay and sand.

	clay		sand	
	μ	σ	μ	σ
^{240}Pu	9.19	0.4	6.99	0.8
^{236}U	7.99	0.4	1.48	0.8

3.2. Adaptive AMC method

In a probabilistic risk analysis of a radioactive waste repository by AMC method, the following steps are performed:

1. N_v values of the retardation factor are sampled;
2. for each sampling, a Monte Carlo score \tilde{J}_M is computed (M is the batch size);
3. the mean \hat{J}_{N_v} of the N_v Monte Carlo scores \tilde{J}_M is considered as the target value.

It emerges from numerical experiments that, with a moderate batch size, accurate mean values of concentrations are obtained. But the Monte Carlo scores \tilde{J}_M observed are not representative if the batch size is not enough large. This could lead to a wrong estimate of the probability of exceeding some imposed critical concentration, which could arise from regulatory requirements. In Fig. 1, we propose an adaptive AMC method in which the batch size is dynamically increased during successive simulations. To compute Monte Carlo scores after increasing the batch size, it is not necessary to restart the whole process provided that suitable intermediate information (samplings, random walks, truncated Neumann series) are stored. Our algorithm could also be used for a dynamic reduction of the statistical errors.

- ```

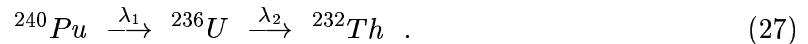
1. Do $i = 1, N_v$
 sampling of parameters (store)
 1.1 Do $j = 1, M$
 radionuclides transport by
 random walks
 End Do
 1.2 store information for later use
 1.3 Intermediate score
 End Do
2. If not satisfied increase M and go to 1.
3. Final score (mean value)
4. Stop

```

Figure 1: Adaptive adjoint Monte Carlo algorithm

## 4. Numerical experiments

The radioactive waste repository is located in a clay layer surrounded by sand layers. The upper aquifer sand layer extends from  $z = -200\text{ m}$  to the upper surface of equation  $z = 10\text{ m}$  where there is no flux. In the clay layer, which extends from  $z = -200\text{ m}$  to  $z = -290\text{ m}$ , the ground-water flow (Darcy velocity) is assumed to be zero. The domain extends horizontally from  $x = 0\text{ m}$  and  $y = 0\text{ m}$  to  $x = 10\,000\text{ m}$  and  $y = 10\,000\text{ m}$ . We assume a band release of radionuclides from the source, which is centered at  $\bar{r} = (2500\text{ m}, 2500\text{ m}, -240\text{ m})$ , and whose total activity is  $3.2 \times 10^{23}\text{ dpy}$  (disintegrations per year). Note that  $10^{23}\text{ dpy} \approx 3 \times 10^{15}\text{ Bq}$ . We consider the following radionuclide chain:



Only the first two elements of the chain are considered in the migration. The last one ( ${}^{232}\text{Th}$ ) is assumed to be stable. The activity proportions of  ${}^{240}\text{Pu}$  and  ${}^{236}\text{U}$  in the source are 0.9999 and  $10^{-4}$ , respectively. The other parameters are given as in Table 2. The target value is the cumulative activity  $\mathcal{A}$  of  ${}^{236}\text{U}$  at the upper clay-sand interface ( $z = -200\text{ m}$ ) after  $3.0001 \times 10^7$  years. The effects of the uncertainty on the value of the retardation factors are taken into account. We are interested in estimating the probability of exceeding given radionuclide activity threshold  $\mathcal{A}_0$ :  $P(\mathcal{A} \geq \mathcal{A}_0)$ . The computations are carried out by means of the TRACKS code [7].

For any number of parameter samplings (retardation factors)  $N_v$  and batch size  $M$ ,  $P(\mathcal{A} \geq \mathcal{A}_0)$  is estimated from the set of scores observed together with their relative frequencies. The results of our experiments are reported in Tables 3-5. Each score is given in the form  $a \pm b$  where  $a$  denotes the average computed while  $b$  stands for the statistical uncertainty at 90 % statistical confidence level [5,6]. We have the following comments.

- The global mean score is almost independent of (reasonable values of) the batch  $M$  and the number of parameter samplings  $N_v$ . All the activity estimates observed belong to the confidence interval [11.24 , 13.06] whose mean value is 12.15.

Table 2: Radioactive decay constant ( $\lambda_i$ ) in  $yr^{-1}$ , uncertain retardation factors ( $R_i$ ), Darcy velocity ( $q1_z$ ) in  $m/yr$ , porosity ( $\theta$ ), molecular diffusion ( $D_m$ ) in  $m^2/yr$ , and dispersivity (in  $m$ ).

| radionuclide                | $\lambda_i$             | $R_i$  |       |
|-----------------------------|-------------------------|--------|-------|
|                             |                         | clay   | sand  |
| $^{240}Pu$                  | $1.0250 \times 10^{-4}$ | 10 670 | 1 500 |
| $^{236}U$                   | $2.8860 \times 10^{-8}$ | 3 200  | 6     |
| ground-water Darcy velocity |                         | 0.     | 2.27  |
| porosity                    |                         | 0.3    | 0.3   |
| molecular diffusion         |                         | 0.010  | 0.073 |
| dispersivity                |                         | 0      | 40    |

Table 3:  $M = 10000$ ,  $N_v$  variable, Activity unit:  $10^{23} dpy$ ,  $\mathcal{A}_0 = 20, 30, 40$ .

|       |                  | $P(\mathcal{A} \geq \mathcal{A}_0)$ for $\mathcal{A}_0 =$ |        |    |
|-------|------------------|-----------------------------------------------------------|--------|----|
| $N_v$ | Activity         | 20                                                        | 30     | 40 |
| 1000  | $12.03 \pm 0.25$ | 0.066                                                     | 0.0000 | 0. |
| 2000  | $12.16 \pm 0.18$ | 0.072                                                     | 0.0010 | 0. |
| 3000  | $12.11 \pm 0.15$ | 0.069                                                     | 0.0013 | 0. |
| 5000  | $12.06 \pm 0.12$ | 0.071                                                     | 0.0022 | 0. |
| 10000 | $12.04 \pm 0.08$ | 0.071                                                     | 0.0017 | 0. |

Table 4:  $M = 20000$ ,  $N_v$  variable, Activity unit:  $10^{23} dpy$ ,  $\mathcal{A}_0 = 20, 30, 40$ .

|       |                  | $P(\mathcal{A} \geq \mathcal{A}_0)$ for $\mathcal{A}_0 =$ |        |        |
|-------|------------------|-----------------------------------------------------------|--------|--------|
| $N_v$ | Activity         | 20                                                        | 30     | 40     |
| 1000  | $12.59 \pm 0.28$ | 0.095                                                     | 0.0040 | 0.0000 |
| 2000  | $12.73 \pm 0.20$ | 0.102                                                     | 0.0060 | 0.0000 |
| 3000  | $12.69 \pm 0.16$ | 0.098                                                     | 0.0063 | 0.0003 |
| 5000  | $12.62 \pm 0.13$ | 0.099                                                     | 0.0068 | 0.0002 |
| 10000 | $12.60 \pm 0.09$ | 0.099                                                     | 0.0061 | 0.0001 |

- When we keep the batch size  $M$  unchanged while we let the number of parameter samplings  $N_v$  vary from 1000 to 10000, it is clear from Tables 3 and 4 that  $P(\mathcal{A} \geq \mathcal{A}_0)$  weakly depends on  $N_v$ . There is however a significant discrepancy between the estimated probabilities for  $M = 10000$  and  $M = 20000$ .
- Too small values of the number of parameter samplings  $N_v$  and, to a large extent, unsuitable values of the batch size  $M$ , may give rise to a rough, or even a completely wrong, probability estimate for exceeding given thresholds. For instance, from the third row and the last column of Table 3 we have that  $P(\mathcal{A} \geq 30 \times 10^{23} \text{ dpy}) = 0$  and  $P(\mathcal{A} \geq 40 \times 10^{23} \text{ dpy}) = 0$ . However, both events have obviously non-zero probabilities.
- All the above observations bring out the necessity of dynamically increasing the batch size when probabilities are sought.

Table 5:  $M = 10000$  fixed,  $M$  variable, Activity unit:  $10^{23} \text{ dpy}$ ,  $\mathcal{A}_0 = 20, 30, 40$ .

|         |                  | $P(\mathcal{A} \geq \mathcal{A}_0)$ for $\mathcal{A}_0 =$ |        |        |
|---------|------------------|-----------------------------------------------------------|--------|--------|
| $N_v$   | Activity         | 20                                                        | 30     | 40     |
| 10000   | $12.04 \pm 0.08$ | 0.071                                                     | 0.0017 | 0.0000 |
| 20000   | $12.60 \pm 0.09$ | 0.099                                                     | 0.0061 | 0.0001 |
| 100 000 | $11.33 \pm 0.09$ | 0.074                                                     | 0.0066 | 0.0003 |
| 120 000 | $12.38 \pm 0.09$ | 0.086                                                     | 0.0066 | 0.0003 |
| 140 000 | $11.31 \pm 0.07$ | 0.048                                                     | 0.0017 | 0.0001 |
| 150 000 | $11.91 \pm 0.08$ | 0.063                                                     | 0.0029 | 0.0001 |
| 160 000 | $12.97 \pm 0.09$ | 0.104                                                     | 0.0083 | 0.0003 |
| 180 000 | $12.17 \pm 0.08$ | 0.078                                                     | 0.0050 | 0.0001 |
| 200 000 | $11.84 \pm 0.08$ | 0.073                                                     | 0.0061 | 0.0003 |

## 5. Concluding remarks

We have proposed an adaptive adjoint Monte Carlo simulation algorithm for the risk analysis of a radioactive waste repository when the uncertainty of hydro-geological parameters are taken into consideration. The batch size is dynamically increased during the computations. This enables us to obtain not only accurate estimates of concentrations at target areas, but also a fair representation of concentration distribution for a given area. Numerical experiments reported show that adaptive AMC algorithm could be successfully used to improve the estimated probability of exceeding some imposed concentration threshold, which could arise from regulatory requirements. Nevertheless, there are a few points that await further investigation. One should find out rules for choosing the starting batch size  $M$ , and rules for increasing the batch size. Appropriate criteria for stopping the process should be designed too.

## References

1. R.D. Burnett, and E.O. Frind. Simulation of contaminant transport in three dimensions. 2. Dimensionality effects. *Water Resources Research*, 23(4):695–705, 1987.
2. G. Dagan. *Flow and Transport in Porous Formations*. Springer-Verlag, New York, 1989.
3. R.A. Freeze. A stochastic-conceptual analysis of one-dimensional ground-water flow in nonuniform homogeneous media. *Water Resources Research*, 11(5):725–741, 1975.
4. L.W. Gelhar. *Stochastic Subsurface Hydrology*. Prentice Hall, New Jersey, 1993.
5. M.H. Kalos, and P.A. Whitlock. *Monte Carlo Methods, Volume 1: Basics*. John Wiley and sons, New-York, 1986.
6. I. Lux, and L. Koblinger. *Monte Carlo Particle Transport Methods : Neutron and Photon Calculations*. CRC Press, 1991.
7. M. Magolomonga Made, and O.F. Smidts. TRACKS.1.0 : A non-analog Monte Carlo transport code for the risk assessment of radioactive repository sites. Users'guide. Université Libre de Bruxelles, July 2003.
8. J. Marivoet. Updating of the Performance Assessment of Geological Disposal of High - Level and Medium Level wastes in the Boom clay formation. Technical Report BLG 634, SCK/CEN - NIRAS/ONDRAF, 1990.
9. K.K. Sabelfeld. *Monte Carlo Methods in Boundary Value Problems*. Springer Series in Computational Physics. Springer-Verlag, Berlin, 1991.
10. Safety Assessment and Feasibility Interim Report (SAFIR) 2. Technical Report, NIRAS/ONDRAF, December 2001.
11. O.F. Smidts. *Analyse probabiliste du risque du stockage de déchets radioactifs par la méthode des arbres d'événements continus*. PhD thesis, Université Libre de Bruxelles, Brussels, 1997.
12. O.F. Smidts. Point and surface estimations by a non-analog Monte Carlo simulation for the transport of radionuclide chains in porous media, *Monte Carlo Methods and Applications*, 4(4):289–318 (1998).
13. O.F. Smidts. Applications of an adjoint Monte Carlo method to the underground migration of radionuclides over large scales, *Annals of Nuclear Energy*, 29:717–750 (2002).
14. O.F. Smidts, and J. Devooght. Analysis of the transport of radionuclide chains in a stochastic geological medium by a biased Monte Carlo simulation. *Nuclear Science and Engineering*, 129:224–245 + corrigendum, 130:164, 1998.
15. O.F. Smidts, and J. Devooght. A non-analog Monte Carlo simulation of transport of radionuclides in a porous medium. *Mathematics and Computers in Simulation*, 47(2–5):461–472, 1998.
16. B.G.J. Thompson, and B. Sagar. The development and application of integrated procedures for post-closure assessment, based upon Monte Carlo simulation: the probabilistic systems assessment (PSA) approach. *Reliability Engineering & System Safety*, 42:125–160, 1993.
17. A.F.B. Tompson, R. Ababou, and L.W. Gelhar. Implementation of the three-dimensional turning bands random field generator. *Water Resources Research*, 25(10):2227–2243, 1989.
18. A.F.B. Tompson, and L.W. Gelhar. Numerical simulation of solute transport in three-dimensional, randomly heterogeneous media. *Water Resources Research*, 26(10):2541–2562, 1990.
19. C. Zheng, and G.D. Bennett. *Applied contaminant transport modeling: Theory and Practice*. John Wiley and Sons, New York, 1995.
20. C. Zheng, and P.P. Wang. MT3DMS: A modular three-dimensional multi-species transport model for simulation of advection, dispersion, and chemical reactions of contaminants in ground-water systems. Documentation and user's guide. Contract Report SERDP-99-1, U.S. Army Engineer Research and Development Center, Vicksburg, MS, 1999.